Articles

Substitution of Aspartic Acid for Methionine-306 in Factor VIIa Abolishes the Allosteric Linkage between the Active Site and the Binding Interface with Tissue Factor

Egon Persson,*,‡ Lars S. Nielsen,§ and Ole H. Olsen||

Vascular Biochemistry and Medicinal Chemistry Research IV, Novo Nordisk A/S, Novo Nordisk Park, DK-2760 Måløv, Denmark, and Molecular Genetics, Novo Nordisk A/S, Novo Allé, DK-2880 Bagsværd, Denmark

Received July 11, 2000; Revised Manuscript Received December 15, 2000

ABSTRACT: The enzyme factor VIIa (FVIIa) triggers the blood coagulation cascade upon association with tissue factor (TF). The TF-induced allosteric enhancement of FVIIa's activity contributes to the procoagulant activity of the complex, and Met-306 in the serine protease domain of FVIIa participates in this event. We have characterized FVIIa variants mutated in position 306 with respect to their ability to be stimulated by TF. The amidolytic activity of FVIIa mutants with Ser, Thr, and Asn in position 306 was stimulated 9-, 12-, and 7-fold, respectively, by soluble TF as compared to 22-fold for wild-type FVIIa. In contrast, the activity of Met306Asp-FVIIa only increased about 2-fold and that of Met306Asp/Asp309Ser-FVIIa increased about 1.5-fold. Modeling suggests that Asp in position 306 prevents the TF-induced stimulation of FVIIa by disrupting essential intermolecular hydrogen bonds. The ability of the FVIIa variants to catalyze factor X activation and the amidolytic activity were enhanced to a similar extent by soluble TF. This indicates that factor X does not promote its own activation through interactions with exosites on FVIIa made accessible upon FVIIa−TF assembly. Met306Asp-FVIIa binds soluble TF with a dissociation constant of 13 nM (about 3-fold higher than that of FVIIa), and, in sharp contrast to FVIIa, its binding kinetics are unaltered after inactivation with D-Phe−Phe−Arg chloromethyl ketone. We conclude that a single specific amino acid replacement, substitution of Asp for Met-306, virtually prevents the TF-induced allosteric changes which normally result in dramatically increased FVIIa activity and eliminates the effect of the active site inhibitor on TF affinity.

Exposure of the membrane protein tissue factor (TF)[1] to blood leads to complex formation with factor VIIa (FVIIa) which triggers blood coagulation (*1*). The interaction between FVIIa and TF involves a large interface with contributions from all extracellular domains of the complex (*2*, *3*). The extended contact area restricts the segmental flexibility of FVIIa and positions the active site at an appropriate distance above the membrane surface (*4*) for cleavage of the physiological substrates factors IX and X (FX). Moreover, free FVIIa is a modestly active enzyme, but upon binding to TF the active conformation of the serine protease domain is stabilized as manifested by the insertion of the N-terminus into the body of the domain (*5*, *6*). A structural change in the N-terminal region upon activation and TF binding has also been demonstrated using a monoclonal antibody (*7*). The allosteric upregulation of the catalytic activity of FVIIa can be detected as a profound increase in the rate of hydrolysis of peptidic ester substrates (*8*). The contributions of many individual residues to the binding energy of the FVIIa−TF interaction and their importance for the biological activity of the complex have been assessed by alanine scanning mutagenesis of both proteins (*9*−*13*). A limited number of the interactive residues are of functional importance. Met-306 in FVIIa appears to be involved in the communication between TF and the catalytic center of FVIIa responsible for the allosteric enhancement of FVIIa's activity (*13*, *14*). Oxidation of Met-306 to the corresponding sulfoxide is sufficient to reduce the specific activity of TF-bound FVIIa (*15*). In addition, a structural difference between TF-bound (*2*, *3*) and free FVIIa (*16*) is found in an α-helical region adjacent to Met-306, corroborating the concept that this residue is instrumental for the regulation of FVIIa activity by TF. However, it remains to be demonstrated whether this

* Corresponding author: Egon Persson, Vascular Biochemistry, Novo Nordisk A/S, Novo Nordisk Park, DK-2760 Måløv, Denmark. Tel: (45) 44 43 43 51. Fax: (45) 44 43 44 17. E-mail: egpe@novonordisk.com.

‡ Vascular Biochemistry, Novo Nordisk A/S.

|| Medicinal Chemistry Research IV, Novo Nordisk A/S.

§ Molecular Genetics, Novo Nordisk A/S.

[1] Abbreviations: BHK, baby hamster kidney; ELISA, enzyme-linked immunosorbent assay; FVII, coagulation factor VII; FVIIa, activated coagulation factor VII; FX, coagulation factor X; FXa, activated coagulation factor X; Gla, γ-carboxyglutamic acid; PAGE, polyacrylamide gel electrophoresis; SPR, surface plasmon resonance; sTF, soluble tissue factor (residues 1−219); TF, tissue factor; vdW, van der Waals.

10.1021/bi001612z CCC: $20.00
Published on Web 02/22/2001

residue is the sole mediator of the allosteric influence of TF on FVIIa.

The recognition and activation of macromolecular substrates, such as FX, by FVIIa−TF involve multiple interactions outside the active site cleft of FVIIa as opposed to the hydrolysis of small pseudosubstrates, which depends exclusively on a mature catalytic machinery. For instance, a TF mutant was found to form a functionally normal complex with FVIIa in terms of amidolytic activity but defective in terms of FX processing (*17*). The γ-carboxyglutamic acid (Gla)-containing domain of FVIIa and FX appears to be involved in several protein−protein interactions required for optimal activation (*18*, *19*). A loop in the second extracellular domain of TF, including residues Lys-165 and Lys-166, has been shown to be important for the ability of the FVIIa−TF complex to activate FX (*20*−*22*). Mutations of the two lysine residues have no effect after removal of the Gla domain of FX, suggesting a direct interaction with this part of the substrate (*23*). Another recognition of the Gla domain of FX involves Arg-36 in TF-bound FVIIa (*24*). Taken together, docking of the FX Gla domain seems to involve a site created by the Gla domain of FVIIa together with the C-terminal domain of TF. An additional substrate exosite has been identified in the protease domain of FVIIa (*13*). Similar to the TF binding interface in the FVIIa protease domain, this exosite region appears to be allosterically connected to the active site of FVIIa. However, TF binding and active site occupancy appear to result in distinct structural alterations (*7*, *25*).

The TF-induced enhancement of FVIIa-catalyzed cleavage of FX is the effect of allosteric changes near the active site as well as macromolecular substrate recognition by a discontinuous, extended binding site formed by both enzyme and cofactor in the FVIIa−TF complex. Herein we have mutated Met-306 in FVIIa to determine whether this residue can be entirely responsible for the FVIIa activity stimulation on TF binding and employed the mutants to shed light on whether FX can promote its own activation through exosite interactions with FVIIa−TF.

EXPERIMENTAL PROCEDURES

Reagents and Standard Methods. The preparation of recombinant wild-type FVIIa and recombinant soluble TF (sTF) were carried out as described (*26*, *27*). Factor VII (FVII) and FVIIa concentrations were determined using a double monoclonal (both recognizing epitopes in the light chain of FVIIa) enzyme-linked immunosorbent assay (ELISA) and sTF concentrations by absorbance measurements at 280 nm using an absorption coefficient of 1.5 for a 1 mg/mL solution. FX and factor Xa (FXa) were from Enzyme Research Laboratories (South Bend, IN), and the chromogenic substrates S-2288 and S-2765 were from Chromogenix (Mölndal, Sweden). Clotting activity was measured in a one-stage assay using FVII-deficient human plasma (Helena Laboratories, Beaumont, TX) and Manchester standard rabbit thromboplastin (Helena BioSciences, Sunderland, U. K.) with pooled normal human plasma as the reference. This assay is predictive for the effects of the FVIIa mutations in a human system because Met-306 and Asp-309 are conserved in rabbit FVII (*28*). SDS−polyacrylamide gel electrophoresis (PAGE) was run on 8−25% gradient gels using the PhastSystem (Amersham Pharmacia Biotech AB, Uppsala, Sweden).

Mutagenesis and Protein Expression. The wild-type FVII expression plasmid pLN174 (*29*) was used as the template for site-directed mutagenesis. M306T- and M306N-FVII were created using the QuikChange kit (Stratagene, La Jolla, CA), and the remaining FVII mutants were made as described (*30*) using the following primers (only sense primers given) with base substitutions in italic and the affected codons underlined: M306T, CCC CGG CTG *ACG* ACC CAG GAC TGC CTG CAG CAG; M306N, CCC CGG CTG *AAC* ACC CAG GAC TGC CTG CAG CAG; M306D, CCC CGT CTA *GAT* ACC CAG GAC TGC CTG CAG CA; M306S, *AGT* ACC CAG GAC TGC CTG CAG CAG TCT AGA AAG GTG GGA GAC TCC CCA AA; M306D/D309S, T CTA *GAT* ACC CAG *TCT* TGC CTG CAG CAG TCA CGG AA. Plasmids were prepared using the QIAprep spin miniprep and QIAfilter plasmid midi kits (Qiagen, Valencia, CA). The cDNA regions encoding the second EGF-like domain and the protease domain of M306D- and M306D/D309S-FVII were verified by sequencing to exclude the presence of additional mutations, whereas the other FVII mutants were sequenced around the mutated sequence (approximately 100 bases downstream and 300 bases upstream) to confirm the introduction of the mutations. Baby hamster kidney (BHK) cells were then transfected with the plasmids. Briefly, 5×10^6 BHK cells were seeded in a T80 bottle the day before and grown in Dulbecco's modified Eagle's medium (DMEM) containing 10% fetal calf serum. 8 micrograms of DNA was mixed with 24 μL of FuGENE6 reagent (Boehringer Mannheim, Germany) in 0.8 mL of DMEM. The mixture was added dropwise to the bottle containing the BHK cells and 20 mL of DMEM. The next day, methotrexate was added to a final concentration of 1 μM. The selection medium (containing methotrexate) was changed every other day, and after approximately two weeks the BHK cells were transferred to a T175 bottle. At confluency, cells were transferred to 3-layer T175 flasks for protein production (*29*).

Mutant Isolation and Activation. Tris (10 mM), EDTA (5 mM), and reduced Triton X-100 (0.1% v/v, Sigma) were added to the harvested media. The pH was adjusted to 8.0 and the conductivity was adjusted to 10 mS/cm before application to a column of Q Sepharose Fast Flow (Amersham Pharmacia Biotech AB, Uppsala, Sweden) equilibrated with 10 mM Tris, pH 8.0, containing 50 mM NaCl and 0.1% Triton X-100. The protein was eluted with a linear gradient of NaCl from 50 mM to 1 M. The fractions were screened using a FVII ELISA and those containing FVII mutant were pooled, followed by the addition of $CaCl_2$ to a final concentration of 10 mM. Further purification was accomplished by affinity chromatography using the monoclonal antibody F1A2 essentially as described (*29*). The eluate from this column was supplemented with 15 mM $CaCl_2$, concentrated using Centriprep-10 and Centricon-10 (Amicon, Beverly, MA) to 0.5−1 mg/mL, and left at ambient temperature for 40−50 h to allow for autoactivation to completely convert FVII to FVIIa. A preactivated FVIIa sample of similar protein concentration left for 72 h showed only 10−15% reduction in activity, and no visible changes in the electrophoretic pattern after reduction had occurred as judged by silver staining of an SDS−polyacrylamide gel. This demonstrates that the activation procedure is not detrimental to the proteins, and because the mutants exist primarily in the

zymogen form at the beginning of the incubation they are exposed to even less autodegradative activity during the activation period than the preactivated sample. The final FVIIa concentration was determined by ELISA.

FVIIa Activity Assays. All proteins were diluted in 50 mM Hepes, pH 7.4, containing 0.1 M NaCl, 5 mM $CaCl_2$, and 0.1% (w/v) bovine serum albumin, prior to analysis. All assays were run in a final volume of 200 μL. The amidolytic activity was monitored for 20 min at 405 nm in a SpectraMax 340 microplate spectrophotometer equipped with the software SOFTmax PRO, version 2.2 (Molecular Devices Corp., Sunnyvale, CA). To measure the amidolytic activity in the absence of sTF, 100 nM of wild-type or mutant FVIIa was mixed with 1 mM S-2288. This analysis was performed both in the absence ($CaCl_2$ replaced by EDTA) and presence of Ca^{2+}. The stimulatory effect of sTF on the amidolytic activity was determined by mixing 10 nM FVIIa variant with different concentrations of sTF (0−3 μM) followed by the addition of 1 mM S-2288.

The effect of sTF on FVIIa-catalyzed FX activation was studied by mixing 10 nM FVIIa, M306D-FVIIa, or M306D/D309S-FVIIa with 0−1000 nM sTF. The reaction was started by adding FX (0.8 μM) and allowed to proceed for 15 min. The activation was terminated with EDTA (final concentration 7 mM), and S-2765 (final concentration 0.5 mM) was added to measure the amount of FXa generated. The FXa activity was corrected for the inherent activity of the FX preparation and of the FVIIa−sTF mixture, and the net amount of FXa was derived from a standard curve (0−5 nM). A modified version of this assay was used to determine the K_m of FVIIa and M306D-FVIIa for FX in the absence and presence of sTF. For this purpose, 10 nM FVIIa variant alone, or 1 nM FVIIa plus 25 nM sTF, or 1 nM M306D-FVIIa plus 200 nM sTF, was incubated with 0−6 μM FX for 15 min.

Surface Plasmon Resonance (SPR) Measurements. The conditions for sTF immobilization (approximately 1000 resonance units) in the Biacore instrument (Biacore AB, Uppsala, Sweden), regeneration of the sTF-coated sensor chip, and evaluation of binding data were as described (*30*, *31*). Wild-type and mutant FVIIa, in the active form and after inhibition with FFR chloromethyl ketone (*32*), was injected for 5 min at a concentration of 30−150 nM in 50 mM Hepes, pH 7.4, containing 0.1 M NaCl, 5 mM $CaCl_2$, and 0.02% Tween 80, followed by a 10-min dissociation phase. The flow rate was 5 μL/min, and the temperature was 25 °C.

Molecular Modeling. To explore possible modes of interaction between the mutated side chain in position 306 in FVIIa and FVIIa−TF, a systematic adiabatic approach was pursued that systematically evaluates a discrete set of side chain conformations. The side chain conformations were generated by constraining the torsional angles of the side chain in question to a discrete set of likely conformers. No solvent molecules were taken into account. The molecular mechanical calculations were performed within the framework of the CHARMM22 modeling package (*33*) using an all hydrogen approach (as described in the template file AMINOH.RTF). Side chain conformations were systematically analyzed by successively constraining all torsional angles for C-C and C-S bonds to 180, 60, and −60 degrees. Each conformation was constructed using torsional harmonic potentials with spring constants of 1000 kcal/mol. After energy minimization, using a steepest descent (SD) method (250 steps) followed by an adopted basis Newton Raphson (ABNR) method (250 steps) with a distance-dependent dielectric ($\epsilon_0 = 10$), the van der Waals (vdW) interaction energy between the side chain in question and protein as well as the total vdW energy was evaluated to exclude side chain conformations that clash with protein. If the total vdW energy as well as the interaction energy between the side chain and the protein were negative, all atoms closer than 6 Å to any atom in side chain 306 were further energy minimized (75 steps of SD followed by 75 steps of ABNR). If the resulting vdW interaction energy was below −10 kcal/mol, the structure was saved for further analysis. The protein structures were taken from the crystal structure of the FVIIa−TF complex (*2*).

RESULTS

Isolation and Characterization of FVIIa Mutants. After purification from approximately 1 L of cell culture medium, the yield of all FVII mutants was in the range of 1−2 mg. The mutants were virtually homogeneous and, after reduction, indistinguishable from wild-type FVII as judged by SDS−PAGE followed by silver staining of the gel (not shown). Autoactivation appeared to commence during the concentration step after purification. After completed activation, the reduced mutants gave two bands on SDS−PAGE identical to those of wild-type FVIIa without visible signs of degradation. The amidolytic activity of the mutants was 60−77% of that of wild-type FVIIa in the presence of calcium and 96−160% in its absence. This demonstrates that the proteins were correctly folded and possess virtually normal intrinsic activity and indicates that Ca^{2+} stimulates some of the mutants to a slightly lesser extent than it does wild-type FVIIa.

Binding of sTF to the FVIIa Mutants and Stimulatory Effect of sTF. The amidolytic activity of the mutants was measured at different sTF concentrations and compared to that of FVIIa. When saturated with sTF, M306T-, M306S-, and M306N-FVIIa had approximately half the activity of wild-type FVIIa (Figure 1, panel A). This is similar to what has been observed with M306A-FVIIa (*13*). In sharp contrast, the activity of M306D- and M306D/D309S-FVIIa was only slightly increased by sTF association. Apparent binding constants derived from the sTF titrations were 99 ± 7 nM for M306S-FVIIa and 105 ± 15 nM for M306N-FVIIa (Figure 1, panel B). The value for FVIIa was about 12-fold lower (8.4 ± 0.7 nM). No reliable binding constant could be obtained for M306D-FVIIa due to the small effect of sTF on the activity. To confirm that M306D-FVIIa actually binds the cofactor, the sTF binding kinetics were investigated using SPR. The equilibrium dissociation constant for the binding of M306D-FVIIa to sTF was about 3-fold higher than that of FVIIa due to a faster dissociation rate (Table 1). Because the activity of M306D-FVIIa was barely stimulated by sTF, it was of particular interest to see whether incorporation of an active site inhibitor increases its affinity for sTF the way it does with FVIIa (*14*, *32*). It turned out that FFR chloromethyl ketone treatment of the mutant had no effect on the binding kinetics (Table 1), and the same was observed with M306D/D309S-FVIIa. The previously described M306A-FVIIa mutant displayed a considerable affinity increase after

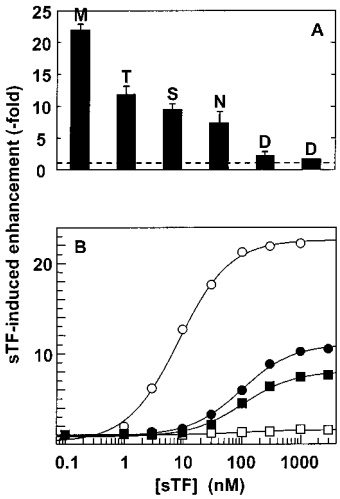

FIGURE 1: Enhancement of the amidolytic activity of the FVIIa variants induced by sTF. Panel A shows the relative activity of the variants in the presence of 1 μM sTF ($n = 3$). Each variant is its own control by arbitrarily setting the activity in the absence of sTF to 1 (dashed line). The letters above the bars indicate the residues occupying position 306. M represents wild-type FVIIa, and the outer right bar shows the stimulation of the double mutant M306D/D309S-FVIIa. The relative activity of representative FVIIa variants at different sTF concentrations is shown in panel B. The results of a representative experiment are shown ($n = 3$). Wild-type FVIIa (○), M306S-FVIIa (●), M306N-FVIIa (■), and M306D-FVIIa (□) at a concentration of 10 nM were mixed with the indicated concentrations of sTF and 1 mM S-2288.

Table 1: sTF Binding Kinetics (mean ± SEM, $n = 3$) of Active and Inhibited FVIIa Variants

	k_{on} ($\times 10^5$ M^{-1} s^{-1})	k_{off} ($\times 10^{-3}$ s^{-1})	K_d (nM)
FVIIa	2.5 ± 0.4	1.2 ± 0.1	4.8
M306D-FVIIa	2.5 ± 0.5	3.3 ± 0.4	13
M306D/D309S-FVIIa	2.9 ± 0.2	6.5 ± 0.2	22
FFR-FVIIa	3.1 ± 0.4	0.3 ± 0.1	1.0
M306D-FFR-FVIIa	3.0 ± 0.4	3.5 ± 0.5	12
M306D/D309S-FFR-FVIIa	2.6 ± 0.1	6.2 ± 0.5	24

inhibitor incorporation (*14*). Together with the sTF stimulation data, this demonstrates that the communication between the binding interface with sTF and the active site has been disrupted in M306D-FVIIa (and in M306D/D309S-FVIIa).

The ability of TF to stimulate the FVIIa variants was also studied using the physiological substrate(s). In a clotting assay, the specific activity of M306D- and M306D/D309S-FVIIa was only 0.1−0.2% of wild-type FVIIa, as compared to 7−8% for M306T- and M306S-FVIIa. This is most likely due to the inability of the mutants to be stimulated by TF, resulting in very slow cleavage of factors X and IX. This was corroborated in a pure system, using FX as the substrate, where M306D-FVIIa responded to sTF with only a 2-fold increase in proteolytic activity (Figure 2), similar to the stimulation observed in the amidolytic activity assay. The proteolytic activity of FVIIa was enhanced about 40-fold by sTF, i.e., slightly more than the 20- to 25-fold increase in amidolytic activity. Hence the presence of sTF does not seem to promote FX activation significantly more than it promotes S-2288 hydrolysis (at least not in solution). The dramatic difference in FX activation between the two FVIIa forms cannot be attributed to differences in K_m. The K_m for FX was determined to be 1.05 ± 0.21 μM for FVIIa, 0.97 ± 0.27 μM for FVIIa−sTF, 0.71 ± 0.10 μM for M306D-FVIIa, and 0.79 ± 0.19 μM for the mutant in complex with sTF. The presence of sTF appeared not to affect K_m for either FVIIa or M306D-FVIIa. From the FX activation experiments, we derived an apparent dissociation constant for binding of FVIIa to sTF of 4.6 ± 1.3 nM, and, due to the poor response to sTF, no reliable value was obtained for M306D-FVIIa.

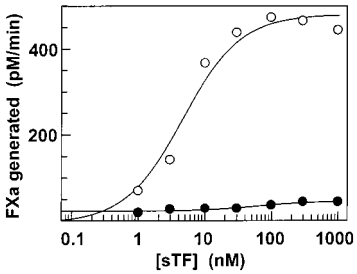

FIGURE 2: sTF-induced stimulation of the rate of FX activation by FVIIa variants. The results of a representative experiment are shown ($n = 3$). Wild-type FVIIa (○) and M306D-FVIIa (●) at a concentration of 10 nM were mixed with the indicated concentrations of sTF and 0.8 μM FX.

Molecular Modeling. Model building provides a rationale as to how the substituted side chains in position 306 in FVIIa may be situated at the interface between FVIIa and TF, i.e., whether they interfere with the surrounding protein structure and alter the interaction region. A range of side chain substitutions were tested using the search procedure described in Experimental Procedures. First, wild-type FVIIa was used to evaluate the feasibility of the approach. The Met side chain orientation observed in the X-ray structure of FVIIa−TF (*2*) was found among the three conformations having the lowest vdW interaction energy with surrounding protein (−18 kcal/mol) without disrupting the local interaction as compared to the X-ray structure (Figure 3, panel A). Phe, Asn, Asp, and Leu were subsequently inserted in position 306 in FVIIa. Interestingly, the Phe side chain interacted tightly (−18.5 kcal/mol) with the protein but altered the interaction region due to its bulkiness (not shown). The Asn (−15 kcal/mol) and Asp (−13.5 kcal/mol) side chains behaved quite differently. The negative charge of Asp disrupted the intimate, stabilizing hydrogen bond network between side chains of TF and side chains/backbone amides of FVIIa (Figure 3, panel B). Thus modeling offers an explanation to the lack of TF-induced stimulation of M306D- and M306D/D309S-FVIIa. To compare Asp to a side chain of approximately the same size (in terms of number of atoms and topology) but with different physicochemical properties the search was performed with a Leu side chain. In this case, the interaction energy was even lower (−19 kcal/mol) than for the Met side chain. Examples of side chain conformations for Leu are shown in Figure 3, panel C.

DISCUSSION

On the basis of the structure of the FVIIa−TF complex, it has been suggested that a loop in FVIIa, succeeding the α-helix comprising residues 307−312, is involved in the TF-induced activity enhancement of FVIIa (*2*). This idea is based on the potential mobility of the loop, which is five residues longer than in the closely related proteases. The mobility might be dictated by the stability of the 307−312 helix, which may be increased by the interactions of Met-306 and

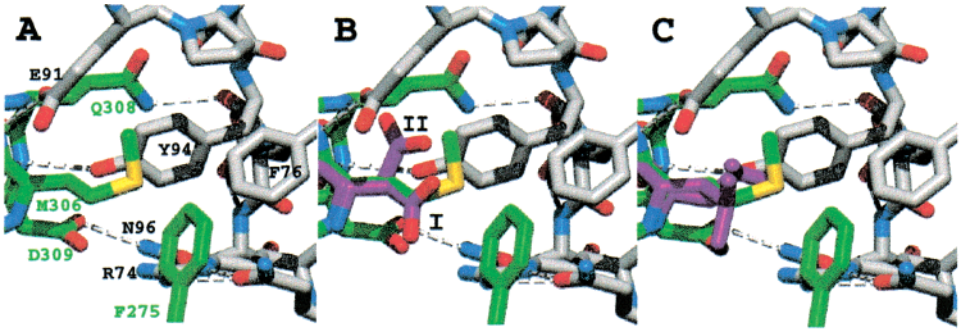

FIGURE 3: The FVIIa−TF interface around Met-306 in FVIIa. The N-terminal part of the 307−312 helix and Phe-275 in FVIIa are shown in green, the region of TF that interacts with FVIIa around Met-306 is in gray (A). Note the hydrogen bond network from Glu-91 in TF to backbone amide of Thr-307 in FVIIa, from Asn-96 in TF to side chain of Asp-309 in FVIIa, and from Tyr-94 in TF to backbone amide of Asp-309 in FVIIa. Modeled side chain conformations are shown for Asp (B) and Leu (C) in position 306 in FVIIa in the FVIIa−TF complex (*2*). The modeled side chains (in magenta) are superimposed on the X-ray structure to illustrate feasible binding modes. In panel B, the two different orientations of the Asp side chain will both potentially disrupt hydrogen bonds.

Asp-309 with TF (*2*). Interestingly, this helix is distorted or unstable in free FVIIa, and we have proposed that the state of the helix regulates FVIIa activity, possibly through the so-called activation domain (*16*). Hence the two hypotheses may represent different ways to express the same allosteric mechanism. They both try to explain the profound influence of TF on FVIIa activity and accommodate the crucial interactions of Met-306 and surrounding residues with TF. The partial reduction in TF-bound FVIIa activity obtained by Ala replacements of Met-306, Asp-309 and adjacent residues in FVIIa does, however, not allow the conclusion that this region is solely responsible, or even the most important, for the TF-induced enhancement of FVIIa activity, especially considering that a similar effect could be obtained by substituting Ala for other residues, for instance Arg-277 (*13*). Partial activity reductions were also observed with three of our FVIIa mutants in position 306. However, the M306A, but not D309A or R277A, mutation eliminated part of the increase in TF affinity induced by active site inhibitor incorporation (*14*). This indicated that position 306 is of outstanding importance and has a unique role in the FVIIa−TF complex. In this report, we show that the enzymatic activity of M306D- and M306D/D309S-FVIIa is almost insensitive to the presence of TF. We also show that the affinity of the mutants for TF is not affected by an active site inhibitor. Because removal of the entire protease domain results in a 30% loss in TF binding energy [K_d = 1−2 μM (*34*) as compared to 3−4 nM for FVIIa], the subtle loss in binding energy (5%) for M306D-FVIIa as compared to FVIIa suggests that the remaining contacts between the protease domain of the mutant and TF are intact. By substituting Asp for Met-306, we have thus shown for the first time that a single residue, independent of other contact points between TF and FVIIa, may mediate the communication between the TF binding interface and the active site. However, it is evident that not all replacements in position 306 are as detrimental to the TF-induced stimulation of FVIIa, and it is also likely that other residues are able to shut off the allosteric linkage as efficiently as Asp. Although we have demonstrated that the disruption of the interaction of residue 306 with TF suffices to abrogate the stimulatory effect, it cannot be ruled out that other contacts between FVIIa and TF are necessary for maximal enhancement of FVIIa activity. One likely candidate is the interaction between the areas around Arg-277 in FVIIa and Trp-45 in TF (*2*, *13*, *35*).

Modeling offers an explanation to the dramatic effect of substituting Asp for Met in position 306 of FVIIa. In the FVIIa−TF complex (Figure 3, panel A), the side chain of Met-306 has a tight hydrophobic interaction with Tyr-94 in TF which excludes water molecules from this interface. The intimate hydrogen bond network between the N-terminal part of the 307−312 helix and TF is disrupted by the negative charge of the modeled Asp side chain in position 306 (Figure 3, panel B). In one conformation (I) the Asp side chain interacts with Asp-309 in FVIIa, thereby disrupting a hydrogen bond between Asp-309 and Asn-96 in TF. In another conformation (II), the Asp in position 306 disrupts the hydrogen bonds between Thr-307 in FVIIa and Glu-91 in TF and between Asp-309 in FVIIa and Tyr-94 in TF. The observed lack of stimulation of the M306D-FVIIa mutant by TF supports the hypothesis that stabilization of the 307−312 helix by a few TF contacts is of great importance for the activity of FVIIa. The smaller impact of Asn in position 306 in FVIIa can be explained by the lack of negative charge. When it comes to the smaller side chains Ser and Thr, it is apparent that they are not as capable of breaking hydrogen bonds. In addition, due to the smaller size of these side chains water molecules can easily penetrate and interfere with the hydrogen bonds. Modeling of Leu in position 306 in FVIIa generated side chain conformations that fitted very well into the FVIIa−TF interface (Figure 3, panel C). Interestingly enough, bovine FVIIa actually has Leu in position 306 (*36*), and bovine TF has Phe in position 94 (*37*). The other side chains in the vicinity of residue 306 in FVIIa are identical in the bovine and human systems. This means that the hydrogen bond between Tyr-94 in human TF and Asp-309 in human FVIIa has been replaced by an equally stabilizing hydrophobic interaction between Phe-94 and Leu-306 in the bovine system. Analogous to the human FVIIa−TF complex, this interaction will exclude water molecules from penetrating the interface between bovine FVIIa and TF.

The allosteric regulation of enzyme activity and specificity via exosite interactions with cofactors, substrates, and inhibitors appears to be a common theme among the clotting factors and not unique for FVIIa. For instance, thrombin possesses several such control sites that have been shown to be utilized by thrombomodulin, hirugen, and thrombin

receptor peptide (*38*−*40*). There is reason to believe that the regulation of for instance factors IXa and Xa is equally elaborate.

ACKNOWLEDGMENT

We thank Helle Bak, Anette Østergaard, and Lone Therkelsen for expert technical assistance. We also thank Mårten Steen for his valuable contributions.

REFERENCES

1. Davie, E. W., Fujikawa, K., and Kisiel, W. (1991) *Biochemistry 30*, 10363−10370.
2. Banner, D. W., D'Arcy, A., Chène, C., Winkler, F. K., Guha, A., Konigsberg, W. H., Nemerson, Y., and Kirchhofer, D. (1996) *Nature 380*, 41−46.
3. Zhang, E., St. Charles, R., and Tulinsky, A. (1999) *J. Mol. Biol. 285*, 2089−2104.
4. McCallum, C. D., Hapak, R. C., Neuenschwander, P. F., Morrissey, J. H., and Johnson, A. E. (1996) *J. Biol. Chem. 271*, 28168−28175.
5. Higashi, S., Nishimura, H., Aita, K., and Iwanaga, S. (1994) *J. Biol. Chem. 269*, 18891−18898.
6. Petersen, L. C., Persson, E., and Freskgård, P.-O. (1999) *Eur. J. Biochem. 261*, 124−129.
7. Dickinson, C. D., Shobe, J., and Ruf, W. (1998) *J. Mol. Biol. 277*, 959−971.
8. Pedersen, A. H., Nordfang, O., Norris, F., Wiberg, F. C., Christensen, P. M., Moeller, K. B., Meidahl-Pedersen, J., Beck, T. C., Norris, K., Hedner, U., and Kisiel, W. (1990) *J. Biol. Chem. 265*, 16786−16793.
9. Schullek, J. R., Ruf, W., and Edgington, T. S. (1994) *J. Biol. Chem. 269*, 19399−19403.
10. Ruf, W., Schullek, J. R., Stone, M. J., and Edgington, T. S. (1994) *Biochemistry 33*, 1565−1572.
11. Ruf, W., Kelly, C. R., Schullek, J. R., Martin, D. M. A., Polikarpov, I., Boys, C. W. G., Tuddenham, E. G. D., and Edgington, T. S. (1995) *Biochemistry 34*, 6310−6315.
12. Kelley, R. F., Costas, K. E., O'Connell, M. P., and Lazarus, R. A. (1995) *Biochemistry 34*, 10383−10392.
13. Dickinson, C. D., Kelly, C. R., and Ruf, W. (1996) *Proc. Natl. Acad. Sci. U.S.A. 93*, 14379−14384.
14. Dickinson, C. D., and Ruf, W. (1997) *J. Biol. Chem. 272*, 19875−19879.
15. Kornfelt, T., Persson, E., and Palm, L. (1999) *Arch. Biochem. Biophys. 363*, 43−54.
16. Pike, A. C. W., Brzozowski, A. M., Roberts, S. M., Olsen, O. H., and Persson, E. (1999) *Proc. Natl. Acad. Sci. U.S.A. 96*, 8925−8930.
17. Lee, G. F., and Kelley, R. F. (1998) *J. Biol. Chem. 273*, 4149−4154.
18. Neuenschwander, P. F., and Morrissey, J. H. (1994) *J. Biol. Chem. 269*, 8007−8013.
19. Rezaie, A. R., Neuenschwander, P. F., Morrissey, J. H., and Esmon, C. T. (1993) *J. Biol. Chem. 268*, 8176−8180.
20. Roy, S., Hass, P. E., Bourell, J. H., Henzel, W. J., and Vehar, G. A. (1991) *J. Biol. Chem. 266*, 22063−22066.
21. Ruf, W., Miles, D. J., Rehemtulla, A., and Edgington, T. S. (1992) *J. Biol. Chem. 267*, 6375−6381.
22. Ruf, W., Miles, D. J., Rehemtulla, A., and Edgington, T. S. (1992) *J. Biol. Chem. 267*, 22206−22210.
23. Huang, Q., Neuenschwander, P. F., Rezaie, A. R., and Morrissey, J. H. (1996) *J. Biol. Chem. 271*, 21752−21757.
24. Ruf, W., Shobe, J., Rao, S. M., Dickinson, C. D., Olson, A., and Edgington, T. S. (1999) *Biochemistry 38*, 1957−1966.
25. Shobe, J., Dickinson, C. D., and Ruf, W. (1999) *Biochemistry 38*, 2745−2751.
26. Thim, L., Bjoern, S., Christensen, M., Nicolaisen, E. M., Lund-Hansen, T., Pedersen, A., and Hedner, U. (1988) *Biochemistry 27*, 7785−7793.
27. Freskgård, P.-O., Olsen, O. H., and Persson, E. (1996) *Protein Sci. 5*, 1531−1540.
28. Brothers, A. B., Clarke, B. J., Sheffield, W. P., and Blajchman, M. A. (1993) *Thromb. Res. 69*, 231−238.
29. Persson, E., and Nielsen, L. S. (1996) *FEBS Lett. 385*, 241−243.
30. Persson, E., Olsen, O. H., Østergaard, A., and Nielsen, L. S. (1997) *J. Biol. Chem. 272*, 19919−19924.
31. Persson, E. (1996) *Haemostasis 26*, Suppl. 1, 31−34.
32. Sørensen, B. B., Persson, E., Freskgård, P.-O., Kjalke, M., Ezban, M., Williams, T., and Rao, L. V. M. (1997) *J. Biol. Chem. 272*, 11863−11868.
33. Brooks, B. R., III, Bruccoleri, R. E., Olafsen, B. D., States, D. J., Swaminthan, S., and Karplus, M. (1983) *J. Comput. Chem. 4*, 187−217.
34. Persson, E. (1997) *FEBS Lett. 413*, 359−363.
35. Kelly, C. R., Schullek, J. R., Ruf, W., and Edgington, T. S. (1996) *Biochem. J. 315*, 145−151.
36. Takeya, H., Kawabata, S., Nakagawa, K., Yamamichi, Y., Miyata, T., Iwanaga, S., Takao, T., and Shimonishi, Y. (1988) *J. Biol. Chem. 263*, 14868−14877.
37. Takayenoki, Y., Muta, T., Miyata, T., and Iwanaga, S. (1991) *Biochem. Biophys. Res. Commun. 181*, 1145−1150.
38. Ye, J., Esmon, N. L., Esmon, C. T., and Johnson, A. E. (1991) *J. Biol. Chem. 266*, 23016−23021.
39. Liu, L.-W., Vu, T.-K. H., Esmon, C. T., and Coughlin, S. R. (1991) *J. Biol. Chem. 266*, 16977−16980.
40. Vijayalakshmi, J., Padmanabhan, K. P., Mann, K. G., and Tulinsky, A. (1994) *Protein Sci. 3*, 2254−2271.

BI001612Z